Simultaneous Wireless Information and Power Transfer in K-tier Heterogeneous Cellular Networks

Sunila Akbar, *Student Member, IEEE,* Yansha Deng, *Member, IEEE,* Arumugam Nallanathan, *Senior Member, IEEE,* Maged Elkashlan, *Member, IEEE,* and A. Hamid Aghvami, *Fellow, IEEE*

***Abstract*—In this paper, we develop a tractable model for joint downlink (DL) and uplink (UL) transmission of K-tier heterogeneous cellular networks (HCNs) with simultaneous wireless information and power transfer (SWIPT) for efficient spectrum and energy utilization. In the DL, the mobile users (MUs) with power splitting receiver architecture decode information and harvest energy based on SWIPT. While in the UL, the MUs utilize the harvested energy for information transmission. Since cell association greatly affects the energy harvesting in the DL and the performance of wireless powered HCNs in the UL, we compare the DL and the UL performance of a random MU in HCNs with nearest base station (NBS) cell association to that with maximum received power (MRP) cell association. We first derive the DL average received power for the MU with the NBS and the MRP cell associations. To evaluate the system performance, we then derive the outage probability and the average ergodic rate in the DL and the UL of a random MU in HCNs with the NBS and the MRP cell associations. Our results show that increasing the small cell base station (BS) density, the BS transmit power, the time allocation factor, and the energy conversion efficiency, weakly affect the DL and UL performance of both cell associations. However, the UL performance of both cell associations can be improved by increasing the fraction of the DL received power used for energy harvesting.**

***Index Terms*—Simultaneous wireless information and power transfer, heterogeneous cellular networks, energy efficiency, spectral efficiency, stochastic geometry.**

I. Introduction

ENERGY efficiency is envisioned as one of the major challenges in the design of fifth generation (5G) systems considering the ever-growing energy consumption [2], and the harmful impact on the environment [3]. At the same time, due to the dramatic increase in the multimedia applications along with the emerging future applications, such as smart cities, health monitoring devices, and driverless cars, the 5G system will require much higher capacity and spectrum efficiency [4]. Radio frequency wireless power transfer (RF-WPT) is an emerging technology which enables the wireless devices to harvest energy from the RF signals for their information processing and transmission, therefore provides efficient energy utilization [5, 6]. Recently, simultaneous wireless information and power transfer (SWIPT) technique has emerged as a novel research direction, which provides significant gains in terms of spectral efficiency and energy consumption by transmitting information and energy via the same signal [7]. Moreover, SWIPT not only offers a low cost option for energy harvesting with no requirement of additional infrastructure at the transmitter side, but also provides better interference control unlike conventional RF-WPT [8].

More recently, there has been an increasing interest in enhancing network capacity via the deployment of small cell base stations (BSs) (e.g., micro, pico, and femto) underlying the conventional macrocell BSs, namely, heterogeneous cellular networks (HCNs). The HCNs boost the network capacity through a better spatial resource reuse [9–11], but the challenge is the resulting increased interference [12–14]. The densely deployed BSs make HCNs attractive for efficient RF-WPT, since the distance between the mobile user (MU) and the BS in HCNs is much shorter than that in homogeneous macrocell networks. Moreover, the aggregate interference in HCNs due to full frequency reuse could be a supplementary energy source. Self-sustained low-cost SWIPT technique can boost the spectrum and energy efficiency while making use of the interference in HCNs.

A. Related Work and Motivations

1) Energy Harvesting in Wireless Powered Communication Networks: Lately, energy harvesting in wireless powered communication networks (WPCNs) has received considerable attention, where wireless devices harvest energy from the ambient RF signals in the wireless network. The work in [15] proposed *'harvest then transmit'* protocol in single-antenna WPCN, where MUs harvest energy in the downlink (DL) for transmitting the uplink (UL) information. The work in [16] studied the energy beamforming design with transmit power control to maximize the UL throughput performance in multi-antenna WPCN. The work in [7] highlighted the potential benefits of SWIPT in resource allocation algorithms and cognitive radio networks. Furthermore, WPCN designs are developed for user cooperation [17], full duplex (FD) network [18], massive multiple input multiple output (MIMO) system [19], and cognitive relay network [20].

2) Energy Harvesting in Wireless Cellular Networks: In [21], RF signal transmitted by primary users was used to power the secondary users in cognitive radio network. In [22], the device to device (D2D) communication was powered by the energy harvested from the concurrent DL transmissions

Manuscript received Oct. 12, 2015; revised Feb. 18, 2016; accepted May 10, 2016. This work was supported by the UK Engineering and Physical Sciences Research Council (EPSRC) with Grant No. EP/M016145/1. This paper was presented in part at the IEEE Global Communications Conference, San Diego, CA, USA, December 2016 [1]. The editor coordinating the review of this manuscript and approving it for publication was Dr. Mehdi Bennis.

S. Akbar, Y. Deng, A. Nallanathan, and H. Aghvami are with the Department of Informatics, King's College London, London, UK (e-mail: {sunila.akbar, yansha.deng, arumugam.nallanathan, hamid.aghvami}@kcl.ac.uk).

M. Elkashlan is with Queen Mary University of London, London E1 4NS, UK (e-mail: maged.elkashlan@qmul.ac.uk).

of the macro BSs. In [23], the power beacons (PBs) were deployed in the cellular network to power the MUs for the UL information transmission, but the deployment of dedicated PBs incur additional operation and maintenance costs. The work in [24] studied RF-WPT in the DL for UL information transmission in K-tier HCNs. In [25], the UL transmission of MUs are powered by the ambient interference. However, it has been mentioned in [26] that harvesting energy from the non-dedicated ambient interference signals could be unstable and unreliable. Applying SWIPT in HCNs can provide stable and reliable energy for MUs by harvesting energy from the dedicated serving BS (similar to PBs), as well as from the DL interference signals at no extra cost.

3) Modeling of Wireless Powered HCNs: Recently, modeling and analysis of HCNs using stochastic geometry has been validated to provide tractable yet accurate performance bounds [27]. A crucial factor in modeling the wireless powered HCNs is cell association which substantially affects the network performance [28]. The UL cell association in wireless powered HCNs has been studied in [29] and [25], where the MUs are powered by the harvested energy from the ambient RF signals. In [29], the UL cell association was based on nearest BS (NBS) cell association, while in [25], it was based on flexible cell association.

B. Contributions and Organization

Motivated to jointly support energy sustainability and high throughput performance, this work aims to integrate SWIPT with HCNs. We use SWIPT in the DL transmission of HCNs where the MUs with no built-in power supply harvest energy and decode information. The MUs then utilize the harvested energy for information transmission in the UL. The NBS cell association both in the DL and the UL is an optimal approach for the proposed HCN due to the following reasons: 1) the low path loss in the UL information transmission as was considered in [29] for wireless powered HCNs, 2) the simple implementation with no system overheads for averaging the received power within a measurement period as with the maximum received power (MRP) cell association, and 3) the design and operation of the logical, transport, and physical channel is less complicated in the coupled cell association, where the MU associates with the same BS in both the DL and UL [30]. Moreover, to study the impact of cell association on SWIPT based wireless powered HCNs, we compare the DL and the UL performance of the proposed HCN with the NBS cell association to that with the conventional MRP cell association.

The main contributions of the paper are summarized as follows:

- Using stochastic geometry, we present the analytical model for SWIPT in HCNs with the NBS and the MRP cell associations, in both DL and UL. We derive the closed-form expression for the DL average received power at the typical MU with the NBS and the MRP cell associations which plays a pivotal role in the UL performance evaluation.
- We derive the analytical expressions for the DL outage probability and the DL average ergodic rate with the NBS and the MRP cell associations. We find that the DL performance of a random MU in HCNs with the NBS cell association can achieve comparable performance to that with the MRP cell association. Our results show that increasing the small cell BS density improves the DL performance of macrocell and picocell MUs with the NBS cell association, whereas has little impact on that with the MRP cell association.
- We evaluate the UL performance in terms of the UL outage probability and the UL average ergodic rate for the NBS and the MRP cell associations. Interestingly, the UL performance of a random MU in HCNs with the NBS cell association is comparable to that with the MRP cell association. We find that increasing the small cell BSs improves the UL performance of both macrocell and picocell MUs with the NBS cell association, whereas degrades that with the MRP cell association.

The rest of the paper is organized as follows. In Section II, we present the system model of SWIPT in HCNs. In Section III, we derive the DL average received power for the NBS and the MRP cell associations. We then evaluate the network performance in terms of the DL and the UL outage probabilities, and the DL and the UL average ergodic rates for the NBS and the MRP cell association in Section IV. Finally, the numerical results are discussed in Section V before the paper is concluded in Section VI.

II. System Model

A. Network Model

We consider a conventional HCN model with K tiers of BSs spatially distributed in $\mathbb{R}^2$ as a homogeneous Poisson point process (HPPP) Φ_j with spatial density λ_j, BS transmit power P_{t,b_j}, and path loss exponent ℓ_{j}, where $j = 1, \cdots, K$ is the index of the jth tier. The MUs are also modeled as an independent HPPP Φ_{u} with density λ_{u}. We assume MUs with large storage battery which eliminates the randomness of instantaneous received power and provides fixed transmit power [23]. We denote the jth tier BS and jth tier MU as b_j, and u_j, respectively. We denote '$\mathrm{k} \in \{1, \cdots, K\}$'as the index of the tier with which a typical MU is associated, and $b_{\widehat{k}}$ as the typical serving BS in the kth tier.

B. Channel Model

We model the channel path loss over the distance $\|\boldsymbol{x}\|$ as $L_0\|\boldsymbol{x}\|^{-\ell_j}$, where L_0 is the path loss at a reference distance of 1 m. We consider Rayleigh fading with unit mean to model the random channel fluctuations, and the channel coefficients are assumed to be independent and identically distributed across all links. We consider no intra-cell interference, where orthogonal multiple access is employed within a cell. We assume time division duplex (TDD) mode. Furthermore, we assume time division multiple access (TDMA), where several MUs share the same channel in different time slots, thus the BS transmit power is independent of the density of active MUs.

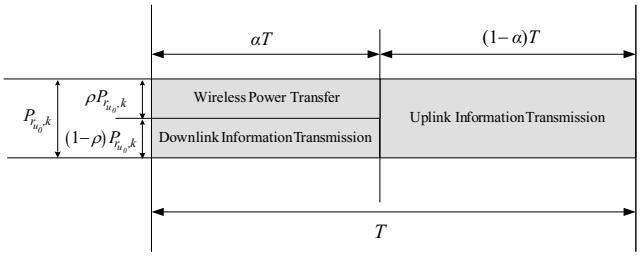

Fig. 1: Frame Structure

C. Transmission Block Model

The transmission block structure is shown in Fig. 1, we assume that the transmission block time is normalized as $T = 1$. A fraction of the block time αT is used for SWIPT, where α $(0 \leq \alpha \leq 1)$ is called the time allocation factor. The remaining portion of time $(1-\alpha)T$ is used for the UL information transmission, which is powered by the energy harvested from the first αT time.

In the DL, the receiver with power splitting architecture splits the received signal for energy harvesting and information decoding. We assume $P_{\mathrm{r_{u_0,k}}}$ as the DL received power at the typical user in the kth tier, a fraction of which $\rho P_{\mathrm{r_{u_0,k}}}$ is used for energy harvesting, where ρ $(0 \leq \rho \leq 1)$ is called the power splitting factor. The remaining fraction of the received power $(1-\rho)P_{\mathrm{r_{u_0,k}}}$ is used for information decoding.

D. Cell Association Model

To ensure low path loss in the UL, we consider the NBS cell association. For a typical MU u_0 located at the origin, the location of the serving nearest BS in the kth tier, $\boldsymbol{x}_{b_{\hat{k}}}$ is given as

$$\boldsymbol{x}_{b_{\hat{k}}}\big|_{\mathrm{NBS}} = \underset{\{\boldsymbol{x}\in\Phi_j\}_{j=1,\cdots,K}}{\operatorname{argmin}} \|\boldsymbol{x}\|, \tag{1}$$

where $\|\boldsymbol{x}\|$ denotes the Euclidean distance between a BS to the typical MU.

We compare the performance of HCNs with the NBS cell association to that with the MRP cell association. In the MRP cell asociation, the MU connects to the BS which offers the maximum (long term averaged) received power to the MU, i.e., small scale fading is ignored, as in [31]. For a typical MU u_0 located at the origin, the location of the serving BS in the kth tier that offers the maximum received power to the typical MU, $\boldsymbol{x}_{b_{\hat{k}}}$ is given as

$$\boldsymbol{x}_{b_{\hat{k}}}\big|_{\mathrm{MRP}} = \underset{\{\boldsymbol{x}\in\boldsymbol{x}_{b_{\hat{j}}}|_{\mathrm{MRP}}\}_{j=1,\cdots,K}}{\operatorname{argmax}} P_{\mathrm{t},b_j}\|\boldsymbol{x}\|^{-\ell_j}. \tag{2}$$

In (2), we have $\boldsymbol{x}_{b_{\hat{j}}}$ as the the location of the BS in the jth tier that offers the maximum received power to the typical MU, given as

$$\boldsymbol{x}_{b_{\hat{j}}}\big|_{\mathrm{MRP}} = \underset{\{\boldsymbol{x}\in\Phi_j\}_{j=1,\cdots,K}}{\operatorname{argmax}} P_{\mathrm{t},b_j}\|\boldsymbol{x}\|^{-\ell_j}, \tag{3}$$

where Φ_j denotes the position sets of BSs in the jth tier.

In the UL information transmission, the typical MU transmits information to the same serving BS of the HCN as in the current cellular networks [28].

E. Wireless Power Transfer Model

A short range propagation model [32] is used for wireless power transfer to avoid the singularity caused by proximity between BSs and MUs i.e., to ensure that the power received at the MU is finite [23]. The received power of a typical MU that is associated to the BS in the kth tier can be written as

$$P_{\mathrm{r_{u_0,k}}} = \underbrace{P_{\mathrm{t},b_{\hat{k}}}\left|h_{b_{\hat{k}}u_0}\right|^2 L_0\left(\max\left\{\left\|\boldsymbol{x}_{b_{\hat{k}},u_0}\right\|,d\right\}\right)^{-\ell_k}}_{I_{b_{\hat{k}}}} + \underbrace{\sum_{j=1}^{K}\sum_{b_j\in\Phi_j\setminus b_{\hat{k}}} P_{\mathrm{t},b_j}\left|h_{b_j u_0}\right|^2 L_0\left(\max\left\{\left\|\boldsymbol{x}_{b_j u_0}\right\|,d\right\}\right)^{-\ell_j}}_{I_{b_x}}, \tag{4}$$

where $I_{b_{\hat{k}}}$ is the useful signal, I_{b_x} is the intercell interference, $d \geq 1$ is a constant, $h_{b_{\hat{k}}u_0}$ is the small-scale fading channel coefficient from the serving BS to the typical MU, $\left\|\boldsymbol{x}_{b_{\hat{k}},u_0}\right\|$ is the distance between the serving BS and the typical MU, $h_{b_j u_0}$ is the small-scale fading interfering channel coefficient from the jth tier BS to the typical MU, and $\left\|\boldsymbol{x}_{b_j u_0}\right\|$ is the distance between the jth tier BS and the typical MU.

F. Downlink Information Transmission Model

In the DL information transmission, a fraction of the received power $(1-\rho)P_{\mathrm{r_{u_0,k}}}$ at the MU is used for information decoding in the αT time.

For the DL analysis, we shift all point processes such that the typical MU is located at the origin. According to Slivnyak's theorem, the distribution of the shifted HPPPs remain the same as the original HPPPs with the same intensities [33]. The signal-to-interference-plus-noise ratio (SINR) of the DL information transmission is given by

$$SINR_k^{DL} = \frac{(1-\rho)\,P_{\mathrm{t},b_{\hat{k}}}\left|h_{b_{\hat{k}}u_0}\right|^2 L_0\left\|\boldsymbol{x}_{b_{\hat{k}}u_0}\right\|^{-\ell_k}}{(1-\rho)\sum_{j=1}^{K}\sum_{b_j\in\Phi_j\setminus b_{\hat{k}}} P_{\mathrm{t},b_j}\left|h_{b_j u_0}\right|^2 L_0\left\|\boldsymbol{x}_{b_j u_0}\right\|^{-\ell_j} + \sigma^2}, \tag{5}$$

where σ^2 is the noise power.

G. Uplink Information Transmission Model

In the UL information transmission, the MUs keep associated with the serving BSs that powered them in the first αT time, and use the harvested energy to transmit the UL information in the $(1-\alpha)T$ time.

We assume large storage MUs so that the randomness of instantaneous received power is suppressed and the large storage provides fixed average received power. We define the

received energy converted into DC for the MU battery in the period αT as $\eta\alpha T\rho\mathbb{E}\{P_{r_{u_0},k}\}$, where $0<\eta<1$ is the energy conversion efficiency. Thus, the signal power for UL information transmission in the period $(1-\alpha)T$ is given as $\phi\mathbb{E}\{P_{r_{u_0},k}\}$, where $\phi=\frac{\eta\rho\alpha}{(1-\alpha)}$.

For the UL analysis, we use Slivnyak's theorem to shift the points of HPPPs such that the serving BS $b_{\widehat{k}}$ is located at the origin. The UL SINR at the serving BS in the kth tier is given by

$$SINR_k^{UL} = \frac{\phi\mathbb{E}\{P_{r_{u_0},k}\}\left|h_{u_0,b_{\widehat{k}}}\right|^2 L_0\left\|\boldsymbol{x}_{u_0,b_{\widehat{k}}}\right\|^{-\ell_k}}{\sum_{j=1}^{K}\sum_{u_j\in\tilde{\Phi}_j\setminus u_0}\phi\mathbb{E}\{P_{r_{u_j},j}\}\left|h_{u_j,b_{\widehat{k}}}\right|^2 L_0\left\|\boldsymbol{x}_{u_j,b_{\widehat{k}}}\right\|^{-\ell_j}+\delta^2}, \tag{6}$$

where $h_{u_0,b_{\widehat{k}}}$ is the small-scale fading channel coefficient from the MU to its serving BS, $\left\|\boldsymbol{x}_{u_0,b_{\widehat{k}}}\right\|$ is the distance between the typical MU and the serving BS, $h_{u_j,b_{\widehat{k}}}$ is the small-scale fading interfering channel coefficient from the jth tier MU u_j to the serving BS, $\left\|\boldsymbol{x}_{u_j,b_{\widehat{k}}}\right\|$ is the distance between the jth tier MU and the serving BS, $\tilde{\Phi}_j$ denotes HPPP corresponding to the interfering MUs in the jth tier, and δ^2 is the noise power.

Based on the model defined in Section II, we aim to derive the analytical expression for the average received power in the DL with the NBS and the MRP cell associations before evaluating the system performance.

III. Analysis of Downlink Power Transfer

To determine the UL transmit power of a typical MU in the kth tier, we derive the average received power at the typical MU with the NBS and the MRP cell associations in Lemma 1 and Lemma 2, respectively.

Lemma 1. *The average received power at the typical MU associated with the BS in the kth tier using NBS cell association is given by*

$$\mathbb{E}\left\{P_{r_{u_0},k}\right\}\big|_{\mathrm{NBS}} = P_{t,b_{\widehat{k}}}L_0(d^{-\ell_k}\chi_1+\chi_2) + 2\pi L_0\sum_{j=1}^{K}P_{t,b_j}\lambda_j\left(\chi_3-\chi_4+\chi_5\right), \tag{7}$$

where

$$\chi_1 = 1-\exp\{\kappa d^2\}, \tag{8}$$

$$\chi_2 = \kappa^{\ell_k/4}d^{-\ell_k/2}\exp\left\{-\frac{1}{2}\kappa d^2\right\}W_{-\ell_k/2,1/2(1-\ell_k/2)}\left(\kappa d^2\right), \tag{9}$$

$$\chi_3 = \frac{\ell_j d^2}{2d^{\ell_j}(\ell_j-2)}[1-\exp\{-\kappa x^2\}], \tag{10}$$

$$\chi_4 = \frac{1}{2\kappa d^{\ell_j}}\gamma(2,\kappa), \tag{11}$$

$$\chi_5 = \frac{\pi\left(\sum_{j=1}^{K}\lambda_j\right)^{(3\ell_j-2)/4}}{\ell_j-2}d^{-\ell_j/2+1}\exp\left\{-\frac{1}{2}\kappa x^2\right\} W_{(\ell_j-2)/4,\ell_j/4}(\kappa d^2), \tag{12}$$

and

$$\kappa = \pi\sum_{j=1}^{K}\lambda_j, \tag{13}$$

where $d\geq 1$ is a constant, defined in (4), $W_{\lambda,\mu}(.)$ is Whittaker function [34], and $\gamma(.,.)$ is lower incomplete gamma function [34].

Proof. See Appendix A. □

Lemma 2. *The average received power at the typical MU associated with the BS in the kth tier using MRP cell association is given by*

$$\mathbb{E}\left\{P_{r_{u_0},k}\right\}\big|_{\mathrm{MRP}} = \frac{P_{t,b_{\widehat{k}}}L_0}{\Upsilon_k}(d^{-\ell_k}\Xi_1+\Xi_2) + \frac{2\pi L_0}{\Upsilon_k}\sum_{j=1}^{K}P_{t,b_j}\lambda_j\left(\Xi_3+(\ell_j-2)^{-1}\Xi_4\right), \tag{14}$$

where

$$\Xi_1 = \int_0^d x\exp\{-\sum_{j=1}^{K}\mu_{k,j}x^{2\ell_k/\ell_j}\}dx, \tag{15}$$

$$\Xi_2 = \int_d^\infty x^{-(\ell_k-1)}\exp\Big\{-\sum_{j=1}^{K}\mu_{k,j}x^{2\ell_k/\ell_j}\Big\}dx, \tag{16}$$

$$\Xi_3 = \int_0^{\theta_{j,k}}\frac{x}{2d^{\ell_j}}\left(\frac{\ell_j d^2}{(\ell_j-2)}-\left(\delta_{j,k}^{DL}\right)^{2/\ell_j}x^{2\ell_k/\ell_j}\right) \exp\Big\{-\sum_{j=1}^{K}\mu_{k,j}x^{2\ell_k/\ell_j}\Big\}dx, \tag{17}$$

$$\Xi_4 = \int_{\theta_{j,k}}^\infty\frac{x\exp\Big\{-\sum\limits_{j=1}^{K}\mu_{k,j}x^{2\ell_k/\ell_j}\Big\}}{\left(\left(\delta_{j,k}^{DL}\right)^{1/\ell_j}x^{\ell_k/\ell_j}\right)^{\ell_j-2}}dx, \tag{18}$$

$$\theta_{j,k} = d^{\ell_j/\ell_k}\left(\delta_{j,k}^{DL}\right)^{-\ell_k}, \tag{19}$$

$$\Upsilon_k = \int_0^\infty r\exp\Big\{-\sum_{j=1}^{K}\mu_{k,j}r^{2\ell_k/\ell_j}\Big\}dr, \tag{20}$$

$$\mu_{k,j} = \pi\lambda_j\left(\delta_{j,k}^{DL}\right)^{2/\ell_j}, \tag{21}$$

and

$$\delta_{j,k}^{DL} = P_{\mathrm{t},b_j}/P_{\mathrm{t},b_k}, \tag{22}$$

where $d\geq 1$ is a constant, defined in (4).

Proof. See Appendix B. □

IV. Performance Evaluations: Analysis

The performance of the DL and the UL transmission of the HCN is characterized by the outage probability and average ergodic rate.

A. Downlink Outage Probability

The DL outage probability is the probability that the instantaneous DL data rate of a randomly selected MU in HCNs is less than the target DL data rate. According to the law of total probability, the DL outage probability of a random MU in K tier HCNs is given by

$$P_{out}^{DL} = \sum_{k=1}^{K} \Lambda_k^{DL} P_{out,k}^{DL}, \tag{23}$$

where Λ_k^{DL} is the probability that a typical MU is associated with the kth tier, and $P_{out,k}^{DL}$ is the DL outage probability of the typical MU associated with the kth tier.

In (23), the probability that a typical MU is associated to the BS in the kth tier with the NBS cell association is given as

$$\Lambda_k\big|_{\mathrm{NBS}} = \left(1 + \frac{\sum_{j=1,j\neq k}^{K} \lambda_j}{\lambda_k}\right)^{-1}, \tag{24}$$

and the probability that a typical MU is associated to the BS in the kth tier with the MRP cell association is given as

$$\Lambda_k\big|_{\mathrm{MRP}} = 2\pi\lambda_k \int_0^{\infty} r \exp\Big\{ -\sum_{j=1}^{K} \mu_{k,j} r^{2\ell_k/\ell_j} \Big\} dr, \tag{25}$$

where $\mu_{k,j}$ is given in (21).

In (23), the DL outage probability for the typical MU at a distance $\left\|\boldsymbol{x}_{b_{\widehat{k}},\mathrm{u}_0}\right\|$ from its associated BS is defined as

$$\begin{aligned} P_{out,k}^{DL}(\mathrm{R}_s) =& \mathbb{E}_{\left\|\boldsymbol{x}_{b_{\widehat{k}},\mathrm{u}_0}\right\|}\Big[\Pr\Big(\alpha \ln\left(1 + SINR_k^{DL}\left(\left\|\boldsymbol{x}_{b_{\widehat{k}},\mathrm{u}_0}\right\|\right)\right) \\ & \leq \mathrm{R}_s\Big)\Big] \\ =& \mathbb{E}_{\left\|\boldsymbol{x}_{b_{\widehat{k}},\mathrm{u}_0}\right\|}\left[\Pr\left(SINR_k^{DL}\left(\left\|\boldsymbol{x}_{b_{\widehat{k}},\mathrm{u}_0}\right\|\right) \leq \beta\right)\right], \end{aligned} \tag{26}$$

where R_s is the rate threshold, and

$$\beta = \mathrm{e}^{\mathrm{R}_s/\alpha} - 1. \tag{27}$$

1) General Case: In this section we provide our general result for the DL outage probability of a typical MU associated with the BS in the kth tier from which the special result for interference-limited case will follow.

Theorem 1. *The DL outage probability of a typical MU associated with the BS in the kth tier using NBS cell association is derived as*

$$\begin{aligned} P_{out,k,NBS}^{DL}(\mathrm{R}_s) =& 1 - 2\kappa \int_0^{\infty} x \exp\Big\{ -\sigma^2\beta\Omega_k^{DL} x^{\ell_k} \\ & - \sum_{j=1}^{K} \pi\lambda_j \Big(\vartheta_{k,j} + x^2\Big)\Big\} dx, \end{aligned} \tag{28}$$

where

$$\vartheta_{k,j} = \mho_{k,j}^{2/\ell_j} \int_{\mho_{k,j}^{-2/\ell_j} x^2}^{\infty} \frac{1}{1 + z^{\ell_j/2}} dz, \tag{29}$$

$$\Omega_k^{DL} = \big((1-\rho) P_{t,b_{\widehat{k}}} L_0\big)^{-1}, \tag{30}$$

and

$$\mho_{k,j} = \beta \delta_{j,k}^{DL} x^{\ell_k}, \tag{31}$$

κ, β, and $\delta_{j,k}^{DL}$ are given in (13)*,* (27)*, and* (22)*, respectively.*

Proof. See Appendix C. □

Theorem 2. *The DL outage probability of a typical MU associated with the BS in the kth tier using MRP cell association is derived as*

$$\begin{aligned} P_{out,k,MRP}^{DL}(\mathrm{R}_s) =& 1 - \frac{1}{\Upsilon_k} \int_0^{\infty} x \exp\Big\{ -\sigma^2\beta\Omega_k^{DL} x^{\ell_k} \\ & - \sum_{j=1}^{K} \pi\lambda_j \Big(\varpi_{k,j} + \left(\delta_{j,k}^{DL}\right)^{2/\ell_j} x^{2\ell_k/\ell_j}\Big)\Big\} dx, \end{aligned} \tag{32}$$

where

$$\varpi_{k,j} = \mho_{k,j}^{2/\ell_j} \int_{\beta^{-2/\ell_j}}^{\infty} \frac{1}{1 + z^{\ell_j/2}} dz, \tag{33}$$

Υ_k, β, $\delta_{j,k}^{DL}$, Ω_k^{DL}, and $\mho_{k,j}$ are given in (20)*,* (27)*,* (22)*,* (30)*, and* (31)*, respectively.*

Proof. See Appendix D. □

2) Interference-Limited Case, Equal Path Loss Exponents $\{\ell_j\} = 4$: In HCNs with high transmit power BSs, the interference dominates the noise. The thermal noise can therefore be neglected in the rest of this section.

Corollary 1. *With $\{\ell_j\} = 4$ and $\sigma^2 = 0$, the DL outage probability of a typical MU associated with the kth tier using NBS cell association is derived as*

$$\begin{aligned} & P_{out,k,NBS}^{DL}(R_s) \\ & = 1 - \frac{\kappa}{\sum_{j=1}^{K} \pi\lambda_j \left(\sqrt{\beta\delta_{j,k}^{DL}} \arctan\left\{\sqrt{\beta\delta_{j,k}^{DL}}\right\} + 1\right)}, \end{aligned} \tag{34}$$

where κ, β, and $\delta_{j,k}^{DL}$ are given in (13)*,* (27)*, and* (22)*, respectively.*

Corollary 2. *With $\{\ell_j\} = 4$ and $\sigma^2 = 0$, the DL outage probability of a typical MU associated with the kth tier using MRP cell association is derived as*

$$\begin{aligned} & P_{out,k,MRP}^{DL}(R_s) \\ & = 1 - \frac{\sum_{j=1}^{K} \lambda_j \sqrt{\delta_{j,k}^{DL}}}{\sum_{j=1}^{K} \lambda_j \sqrt{\delta_{j,k}^{DL}} \left(\left(\sqrt{\beta} \arctan\left\{\sqrt{\beta}\right\}\right) + 1\right)}, \end{aligned} \tag{35}$$

where β and $\delta_{j,k}^{DL}$ are given in (27) *and* (22)*, respectively.*

The expressions in (34) and (35) are in closed-form. We find that the DL outage probability in the interference-limited scenario is independent of the power splitting factor ρ. This is due to the fact that the term $(1-\rho)$ in the $SINR_k^{DL}$ expression in (5) cancels out with $\sigma^2 = 0$.

B. Downlink Average Ergodic Rate

The DL average ergodic rate of a K tier HCNs measures the spectral efficiency of HCNs in the DL. The DL average ergodic rate of a random MU in the K tier HCNs is given by

$$R^{DL} = \sum_{k=1}^{K} \Lambda_k^{DL} R_k^{DL}, \tag{36}$$

where R_k^{DL} is the DL average ergodic rate of a typical MU associated with the kth tier and Λ_k^{UL} is given in (24) for the NBS cell association, and in (25) for the MRP cell association, respectively.

In (36), the DL average ergodic rate for a typical MU at a distance $\left\|\boldsymbol{x}_{b_{\widehat{k}},\mathrm{u}_0}\right\|$ from its associated BS in the kth tier is defined as

$$R_k^{DL} = \mathbb{E}_{\left\|\boldsymbol{x}_{b_{\widehat{k}},\mathrm{u}_0}\right\|}\Bigg[\mathbb{E}_{SINR_k^{DL}}\Big[\alpha \ln\left(1+SINR_k^{DL}\left(\left\|\boldsymbol{x}_{b_{\widehat{k}},\mathrm{u}_0}\right\|\right)\right)\Big]\Bigg]. \tag{37}$$

1) General Case: We now present the general result for the DL average ergodic rate of a typical MU associated with the kth tier followed by the special result for the interference-limited scenario.

Theorem 3. *The DL average ergodic rate of a typical MU associated with the kth tier using NBS cell association is derived as*

$$R_{k,NBS}^{DL} = 2\kappa \int_0^\infty \int_0^\infty x \exp\Big\{-\sigma^2(\mathrm{e}^{t/\alpha}-1)\Omega_k^{DL} x^{\ell_k} - \sum_{j=1}^{K} \pi\lambda_j \Big(\left((\mathrm{e}^{t/\alpha}-1)\delta_{j,k}^{DL} x^{\ell_k}\right)^{2/\ell_j} \int_{((\mathrm{e}^{t/\alpha}-1)\delta_{j,k}^{DL} x^{\ell_k})^{-2/\ell_j} x^2}^{\infty} \frac{1}{1+z^{\ell_j/2}} dz - x^2\Big)\Big\} dt dx, \tag{38}$$

where Ω_k^{DL} and $\delta_{j,k}^{DL}$ are given in (30) *and* (22)*, respectively.*

Proof. See Appendix E. □

Theorem 4. *The DL average ergodic rate of a typical MU associated with the kth tier using MRP cell association is derived as*

$$R_{k,MRP}^{DL} = \frac{1}{\Upsilon_k} \int_0^\infty \int_0^\infty x \exp\Big\{-\sigma^2(\mathrm{e}^{t/\alpha}-1)\Omega_k^{DL} x^{\ell_k} - \sum_{j=1}^{K} \pi\lambda_j \Big(\left((\mathrm{e}^{t/\alpha}-1)\delta_{j,k}^{DL} x^{\ell_k}\right)^{2/\ell_j} \int_{(\mathrm{e}^{t/\alpha}-1)^{-2/\ell_j}}^{\infty} \frac{dz}{1+z^{\ell_j/2}} + \left(\delta_{j,k}^{DL}\right)^{2/\ell_j} x^{2\ell_k/\ell_j}\Big)\Big\} dt dx, \tag{39}$$

where Ω_k^{DL} and $\delta_{j,k}^{DL}$ are given in (30) *and* (22)*, respectively.*

Proof. See Appendix F. □

2) Interference-Limited Case, Equal Path Loss Exponents $\{\ell_j\} = 4$: In the following, we present the DL average ergodic rate of a typical MU associated with the kth tier in HCNs in the interference-limited scenario.

Corollary 3. *With $\{\ell_j\} = 4$ and $\sigma^2 = 0$, the DL averaqe ergodic rate of a typical MU associated with the kth tier using NBS cell association is derived as* (40) *at the top of the next page, where κ and $\delta_{j,k}^{DL}$ are given in* (13) *and* (22)*, respectively.*

Corollary 4. *With $\{\ell_j\} = 4$ and $\sigma^2 = 0$, the DL averaqe ergodic rate of a typical MU associated with the kth tier using MRP cell associations is derived as* (41) *at the top of the next page, where $\delta_{j,k}^{DL}$ is given in* (22)*.*

In these corollaries, the double integral in Theorem 3 and 4 is simplified to a single integral. We find that the DL average ergodic rate in the interference-limited scenario is independent of the power splitting factor due to the fact that with $\sigma^2 = 0$, the term $(1-\rho)$ disappears in the $SINR_k^{DL}$ given in (5).

In the following, we present the UL performance of the HCN which reflects the DL energy harvesting efficiency of SWIPT with the NBS and the MRP cell associations. We characterize the UL performance in terms of the UL outage probability and the UL average ergodic rate.

C. Uplink Outage Probability

The UL outage probability is the probability that the instantaneous UL data rate at the serving BS in HCNs is less than the target UL data rate. The UL outage probability in HCNs is given by

$$P_{out}^{UL} = \sum_{k=1}^{K} \Lambda_k^{UL} P_{out,k}^{UL}, \tag{42}$$

where Λ_k^{UL} is given in (24) for the NBS cell association, and in (25) for the MRP cell association, and $P_{out,k}^{UL}$ is the UL outage probability of a typical MU associated with the kth tier.

In (42), the UL outage probability for a typical MU at a distance $\left\|\boldsymbol{x}_{\mathrm{u}_0,b_{\widehat{k}}}\right\|$ from its associated BS is defined as

$$\begin{aligned} P_{out,k}^{UL}(\mathrm{R}_s) &= \mathbb{E}_{\left\|\boldsymbol{x}_{b_{\widehat{k}},\mathrm{u}_0}\right\|}\Bigg[\Pr\Big((1-\alpha) \ln\left(1+SINR_k^{UL}\left(\left\|\boldsymbol{x}_{b_{\widehat{k}},\mathrm{u}_0}\right\|\right)\right) \le \mathrm{R}_s\Big)\Bigg] \\ &= \mathbb{E}_{\left\|\boldsymbol{x}_{b_{\widehat{k}},\mathrm{u}_0}\right\|}\left[\Pr\left(SINR_k^{UL}\left(\left\|\boldsymbol{x}_{b_{\widehat{k}},\mathrm{u}_0}\right\|\right) \le \Psi\right)\right]. \end{aligned} \tag{43}$$

where

$$\Psi = \mathrm{e}^{\mathrm{R}_s/(1-\alpha)} - 1. \tag{44}$$

$$R_{k,NBS}^{DL}=\int_0^{\infty}\frac{\kappa}{\sum\limits_{j=1}^{K}\pi\lambda_j\left(\sqrt{\left(\mathrm{e}^{t/\alpha}-1\right)\delta_{j,k}^{DL}}\arctan\left\{\sqrt{\left(\mathrm{e}^{t/\alpha}-1\right)\delta_{j,k}^{DL}}\right\}+1\right)}dt, \tag{40}$$

$$R_{k,MRP}^{DL}=\int_0^{\infty}\frac{\sum\limits_{j=1}^{K}\lambda_j\sqrt{\delta_{j,k}^{DL}}}{\sum\limits_{j=1}^{K}\lambda_j\sqrt{\delta_{j,k}^{DL}}\left(\left(\sqrt{\left(\mathrm{e}^{t/\alpha}-1\right)}\arctan\left\{\sqrt{\left(\mathrm{e}^{t/\alpha}-1\right)}\right\}\right)+1\right)}dt, \tag{41}$$

1) General Case: In the following, we derive the general result for the UL outage probability of a typical MU associated with the kth tier.

Theorem 5. *The UL outage probability of a typical MU associated with the kth tier using NBS cell association is derived as*

$$P_{out,k,NBS}^{UL}\left(\mathrm{R}_s\right)=1-2\kappa\int_0^{\infty}x\exp\Bigg\{-\sigma^2\Psi\Omega_k^{UL}x^{\ell_k}-\sum_{j=1}^{K}\left(\zeta_{k,j}^{UL}x^{\frac{2\ell_k}{\ell_j}}\Psi^{\frac{2}{\ell_j}}+\pi\lambda_j x^2\right)\Bigg\}dx, \tag{45}$$

where

$$\Omega_k^{UL}=\left(\phi\mathbb{E}\{P_{r_{\mathrm{u}_0},k}\}L_0\right)^{-1}, \tag{46}$$

$$\zeta_{k,j}^{UL}=\pi\lambda_j\left(\delta_{j,k}^{UL}\right)^{\frac{2}{\ell_j}}\Gamma\left(1+\frac{2}{\ell_j}\right)\Gamma\left(1-\frac{2}{\ell_j}\right), \tag{47}$$

$$\delta_{j,k}^{UL}=\frac{\mathbb{E}\left[P_{r_{\mathrm{u}_j},j}\right]}{\mathbb{E}\left[P_{r_{\mathrm{u}_0},k}\right]}, \tag{48}$$

and Ψ is given in (44)*.*

Proof. The proof follows similar steps to Theorem 1. □

Theorem 6. *The UL outage probability of a typical MU associated with the kth tier using MRP cell association is derived as*

$$P_{out,k,MRP}^{UL}\left(\mathrm{R}_s\right)=1-\frac{1}{\Upsilon_k}\int_0^{\infty}x\exp\Bigg\{-\sigma^2\Psi\Omega_k^{UL}x^{\ell_k}-\sum_{j=1}^{K}\left(\zeta_{k,j}^{UL}x^{\frac{2\ell_k}{\ell_j}}\Psi^{\frac{2}{\ell_j}}+\mu_{k,j}x^{2\ell_k/\ell_j}\right)\Bigg\}dx, \tag{49}$$

where Ψ, Ω_k^{UL}, $\zeta_{k,j}^{UL}$, and $\mu_{k,j}$ are given in (44)*,* (46)*,* (47)*, and* (21)*, respectively.*

Proof. The proof follows similar steps to Theorem 2. □

2) Interference-Limited Case, Equal Path Loss Exponents $\{\ell_j\}=4$: We now present the UL outage probability of a typical MU associated with the kth tier in the interference-limited case.

Corollary 5. *With $\{\ell_j\}=4$ and $\delta^2=0$, the UL outage probability of a typical MU associated with the kth tier using NBS cell association is derived as*

$$P_{out,k,NBS}^{UL}\left(R_s\right)=1-\frac{\kappa}{\sum\limits_{j=1}^{K}\pi\lambda_j\left(\frac{\pi}{2}\sqrt{\delta_{j,k}^{UL}\Psi}+1\right)}, \tag{50}$$

where κ, $\delta_{j,k}^{UL}$, and Ψ are given in (13)*,* (48)*, and* (**??**)*, respectively.*

Corollary 6. *With $\{\ell_j\}=4$ and $\delta^2=0$, the UL outage probability of a typical MU associated with the kth tier using MRP cell association is derived as*

$$P_{out,k,MRP}^{UL}\left(R_s\right)=1-\frac{\sum\limits_{j=1}^{K}\lambda_j\sqrt{\delta_{j,k}^{DL}}}{\sum\limits_{j=1}^{K}\lambda_j\left(\frac{\pi}{2}\sqrt{\delta_{j,k}^{UL}\Psi}+\sqrt{\delta_{j,k}^{DL}}\right)}, \tag{51}$$

where $\delta_{j,k}^{DL}$, $\delta_{j,k}^{UL}$, and Ψ are given in (22)*,* (48)*, and* (**??**)*, respectively.*

We find that the UL outage probabilities for the NBS and the MRP cell associations are independent of the energy conversion efficiency and the power splitting factor. This can be explained by the fact that the term $\phi=\frac{\eta\rho\alpha}{(1-\alpha)}$ in (6) cancels out with $\delta^2=0$.

D. Uplink Average Ergodic Rate

The UL average ergodic rate of a random MU in K tier HCNs is given by

$$R^{UL}=\sum_{k=1}^{K}A_k^{UL}R_k^{UL}, \tag{52}$$

where R_k^{UL} is the UL average ergodic rate of a typical MU associated with the kth tier and Λ_k^{UL} is given in (24) for the NBS cell association, and in (25) for the MRP cell association, respectively.

In (52), the UL average ergodic rate of a random MU located at a distance $\left\|\boldsymbol{x}_{\mathrm{u}_0,b_{\widehat{k}}}\right\|$ from its associated BS in the kth tier is defined as

$$R_k^{UL}=\mathbb{E}_{\left\|\boldsymbol{x}_{\mathrm{u}_0,b_{\widehat{k}}}\right\|}\left[\mathbb{E}_{SINR_k^{UL}}\left[(1-\alpha)\ln\left(1+SINR_k^{UL}\left(\left\|\boldsymbol{x}_{\mathrm{u}_0,b_{\widehat{k}}}\right\|\right)\right)\right]\right]. \tag{53}$$

1) General Case: We now provide the general result for the UL average ergodic rate of a random MU associated with the BS in kth tier.

Theorem 7. *The UL average ergodic rate of a random MU associated with the BS in kth tier using NBS cell association is derived as*

$$R_{k,NBS}^{UL} = 2(1-\alpha)\kappa \int_0^\infty \int_0^\infty \frac{x}{1+t} \exp\Bigg[-\delta^2 \Omega_k^{UL} t x^{\ell_k} - \sum_{j=1}^{K} \left(\zeta_{k,j}^{UL} t^{\frac{2}{\ell_j}} x^{\frac{2\ell_k}{\ell_j}} + \pi \lambda_j x^2 \right) \Bigg] dx dt. \quad (54)$$

where κ, Ω_k^{UL}, and $\zeta_{k,j}^{UL}$ are given in (13)*,* (46)*, and* (47)*, respectively.*

Proof. The proof follows similar steps to Theorem 3. □

Theorem 8. *The UL average ergodic rate of a random MU associated with the BS in kth tier using MRP cell association is derived as*

$$R_{k,MRP}^{UL} = \frac{(1-\alpha)}{\Upsilon_k} \int_0^\infty \int_0^\infty \frac{x}{1+t} \exp\Bigg[-\delta^2 \Omega_k^{UL} t x^{\ell_k} - \sum_{j=1}^{K} \left(\zeta_{k,j}^{UL} t^{\frac{2}{\ell_j}} x^{\frac{2\ell_k}{\ell_j}} + \mu_{k,j} x^{2\ell_k/\ell_j} \right) \Bigg] dx dt, \quad (55)$$

Proof. The proof follows similar steps to Theorem 4. □

2) Interference-Limited Case, Equal Path Loss Exponents $\{\ell_j\} = 4$: We present the UL average ergodic rate of a typical MU associated with the kth tier for the interference-limited network in the following corollaries.

Corollary 7. *With $\{\ell_j\} = 4$ and $\delta^2 = 0$, the UL average ergodic rate of a typical MU associated with the kth tier using NBS cell association is derived as*

$$R_{k,NBS}^{UL} = \int_0^\infty \frac{(1-\alpha)\kappa}{(1+t)\sum_{j=1}^{K} \pi \lambda_j \left(\frac{\pi}{2} \sqrt{\delta_{j,k}^{UL} t} + 1 \right)} dt, \quad (56)$$

where κ and $\delta_{k,j}^{UL}$ are given in (13) *and* (48)*, respectively.*

Corollary 8. *With $\{\ell_j\} = 4$ and $\delta^2 = 0$, the UL average ergodic rate of a typical MU associated with the kth tier using MRP cell association is derived as*

$$R_{k,MRP}^{UL}(R_s) = \int_0^\infty \frac{(1-\alpha)\sum_{j=1}^{K} \lambda_j \sqrt{\delta_{j,k}^{DL}}}{(1+t)\sum_{j=1}^{K} \lambda_j \left(\frac{\pi}{2} \sqrt{\delta_{j,k}^{UL} t} + \sqrt{\delta_{j,k}^{DL}} \right)} dt, \quad (57)$$

where $\delta_{j,k}^{DL}$ and $\delta_{j,k}^{UL}$ are given in (22) *and* (48)*, respectively.*

In the interference-limited scenario, the UL average ergodic rate does not depend on the energy conversion efficiency and the power splitting factor with the NBS and the MRP cell associations. This can be seen in (6) that with $\delta^2 = 0$, the term $\phi = \frac{\eta\rho\alpha}{(1-\alpha)}$ cancels out and $SINR_k^{UL}$ becomes independent of η and ρ.

In the following, we present the global (GL) performance of the HCN which reflects the impact of power splitting factor on the overall (DL+UL) performance. We characterize the GL performance in terms of the GL average ergodic rate. We characterize the GL performance in terms of the GL average ergodic rate.

E. Global Average Ergodic Rate

We define the GL average ergodic rate of a random MU in K tier HCNs as the sum of the DL average ergodic rate and the UL average ergodic rate, as follows

$$R^{GL} = R^{DL} + R^{UL}, \quad (58)$$

where R^{DL} and R^{UL} are given in (36) and (52), respectively. The GL average ergodic rate is defined to find the optimal power splitting factor ρ^* that maximizes the GL average ergodic rate. The evaluation for the exact expression of ρ^* turns out to be intractable, therefore, we numerically evaluate the optimal ρ^* that maximizes R^{GL} in the numerical results.

V. Numerical Results

In this section, we compare the system performance with the NBS cell association to that with the MRP cell association in terms of the DL outage probability, the DL average ergodic rate, the UL outage probability, and the UL average ergodic rate. We plot the DL outage probability, the DL average ergodic rate, the UL outage probability, and the UL average ergodic rate for the NBS cell association using (28), (45), (38), and (54), respectively. We plot the DL outage probability, the DL average ergodic rate, the UL outage probability, and the UL average ergodic rate for the MRP cell association using (32), (39), (49), and (55), respectively. The analytical results are validated by Monte Carlo simulations, where the BSs and the MUs are deployed according to the proposed model for a two-tier HCN. In all the figures, the path loss is assumed to be $L_0 = -38.5$ dB at 1 meter, and the path loss exponents are $\ell_1 = 3.8$ and $\ell_2 = 3.5$. The thermal noise power at the MU and the BS are fixed as $\sigma^2 = \delta^2 = -104$ dB for 10 MHz bandwidth. Unless otherwise stated, the time allocation factor $\alpha = 0.5$, the power splitting factor $\rho = 0.5$, and the energy conversion efficiency $\eta = 0.5$.

A. Effect of Picocell BSs Density and BS Transmit Power

In this subsection, we examine the effect of the density of picocell BSs and the transmit power at the BSs on the DL outage probability, the DL average ergodic rate, the UL outage probability, and the UL average ergodic rate of a random MU in HCNs with the NBS and the MRP cell associations. In Figs. 2, 3, 4, and 5, we set $\lambda_1 = 10^{-3}$ and $R_s = 0.5$ nats/s/Hz.

Downlink Performance: Fig. 2a and Fig. 2b compare the impact of the density of picocell BSs λ_2 and the BS transmit power $P_{t,b}$ of each tier on the DL outage probability with the NBS cell association $P_{out,NBS}^{DL}(R_s)$, to the DL outage

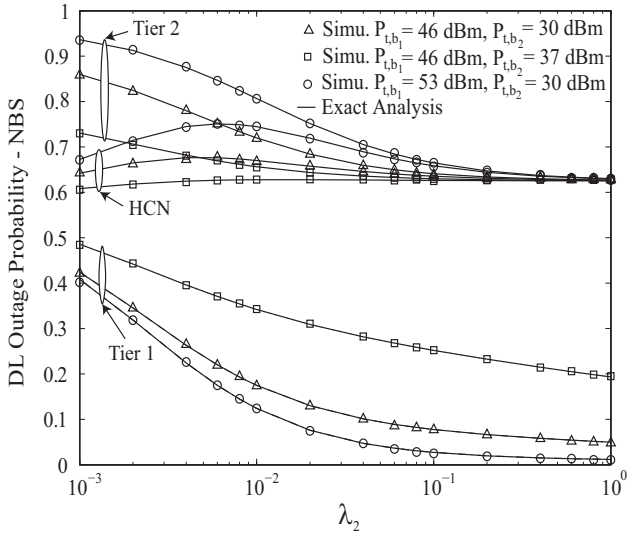

(a) DL outage probability with the NBS cell association.

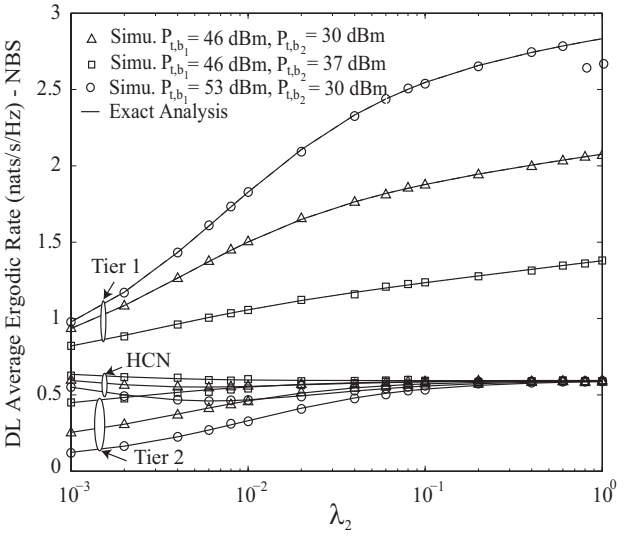

(a) DL average ergodic rate with the NBS cell association.

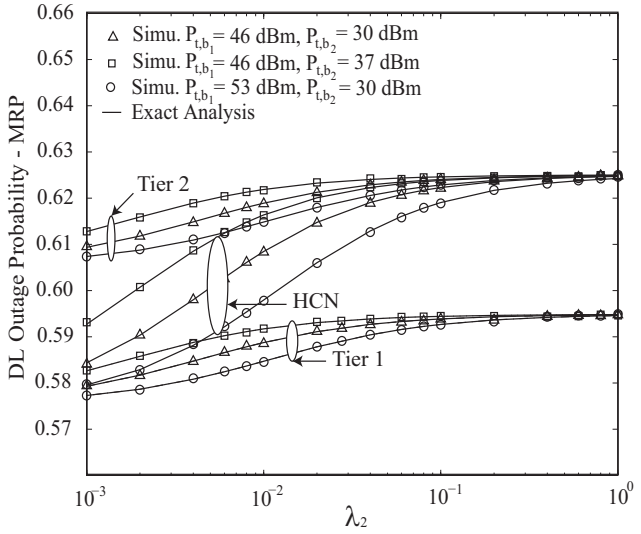

(b) DL outage probability with the MRP cell association.

Fig. 2: Impact of picocell BS density and BS transmit power in a two-tier HCN.

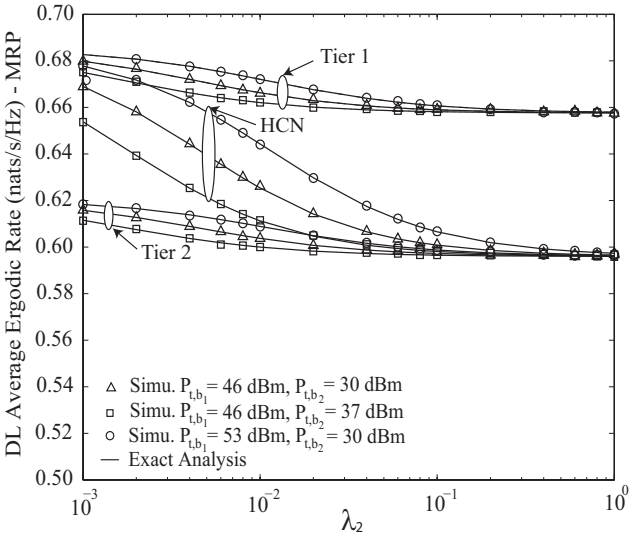

(b) DL average ergodic rate with the MRP cell association.

Fig. 3: Impact of picocell BS density and BS transmit power in a two-tier HCN.

probability with the MRP cell association $P^{DL}_{out,MRP}(R_s)$, respectively. Fig. 3a and Fig. 3b compare the impact of the density of picocell BSs λ_2 and the BS transmit power of each tier on the DL average ergodic rate with the NBS cell association R^{DL}_{NBS}, to the DL aveargе ergodic rate with the MRP cell association R^{DL}_{MRP} respectively.

With the increase of λ_2, $P^{DL}_{out,NBS}$ and R^{DL}_{NBS} improve due to the increase in signal strength at the MU from the nearest serving BS. Interestingly, the increase in λ_2 does not have a significant affect on $P^{DL}_{out,MRP}$ and R^{DL}_{MRP} at both tiers. We also observe that $P^{DL}_{out,NBS}$, R^{DL}_{NBS}, $P^{DL}_{out,MRP}$, and R^{DL}_{MRP} of a random MU in HCNs are approximately the same with the increase in λ_2.

With the increase of $P_{t,b}$ in the kth tier, $P^{DL}_{out,NBS}(R_s)$ and R^{DL}_{NBS} of the kth tier improve, while that of other tiers degrade. This is due to the increased signal power at the MUs in the kth tier, and the increased interference at the MUs of the other tiers. Surprisingly, the increase in $P_{t,b}$ of the kth tier slightly affects $P^{DL}_{out,MRP}(R_s)$ and R^{DL}_{MRP} of both the tiers. Furthermore, it is shown that $P^{DL}_{out,NBS}(R_s)$, R^{DL}_{NBS}, $P^{DL}_{out,MRP}(R_s)$, and R^{DL}_{MRP} of a random MU in HCNs cannot be greatly improved by increasing $P_{t,b}$.

Uplink Performance: Fig. 4a and Fig. 4b show the effect of picocell BS density λ_2 and the BS transmit power $P_{t,b}$ on the UL outage probability with the NBS $P^{UL}_{out,NBS}(R_s)$, to the UL outage probability with the MRP cell association $P^{UL}_{out,MRP}(R_s)$, respectively. Fig. 5a and Fig. 5b compare the impact of the density of picocell BSs λ_2 and the BS transmit power of each tier on the UL average ergodic rate with the NBS cell association R^{UL}_{NBS}, to the UL aveargе ergodic rate

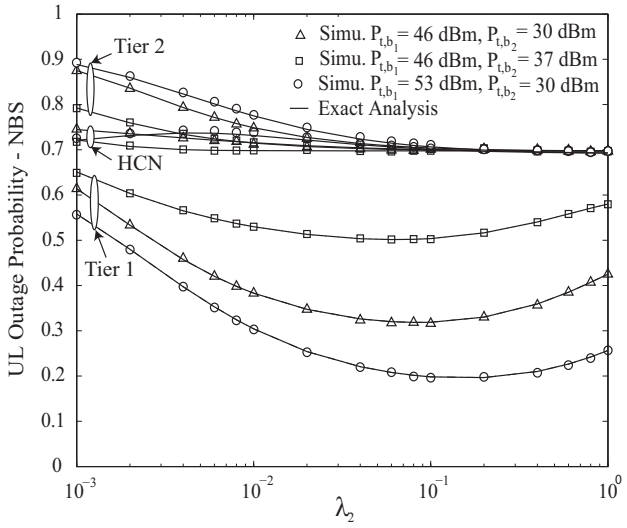

(a) UL outage probability with the NBS cell association.

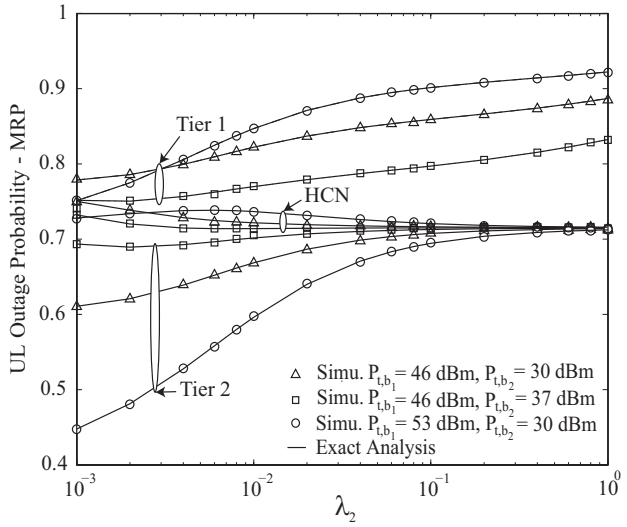

(b) UL outage probability with the MRP cell association.

Fig. 4: Impact of picocell BS density and BS transmit power in a two-tier HCN.

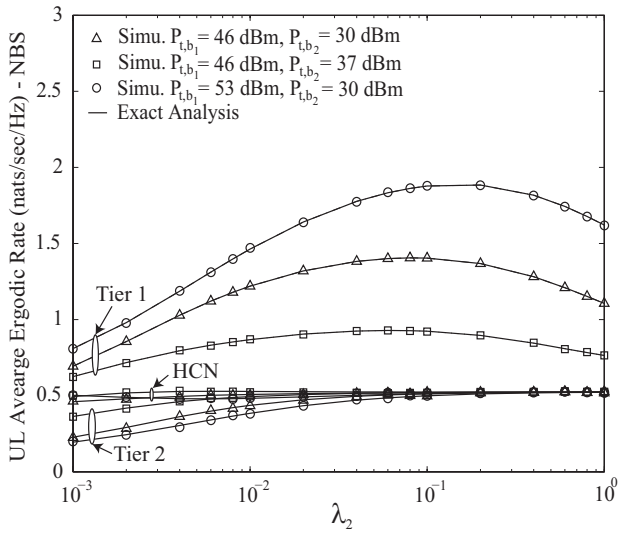

(a) UL average ergodic rate with the NBS cell association.

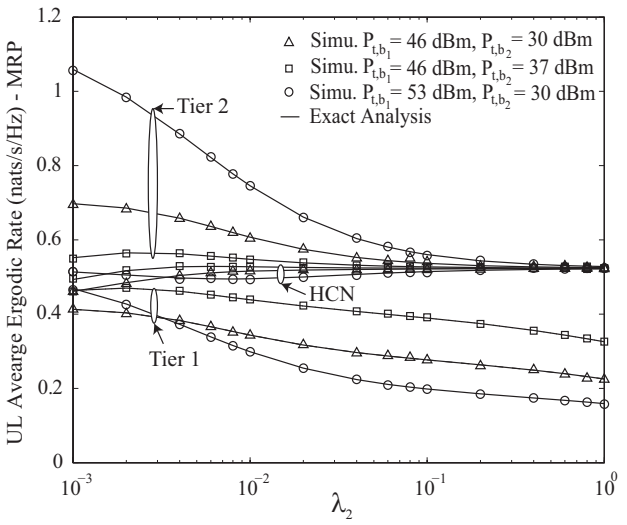

(b) UL average ergodic rate with the MRP cell association.

Fig. 5: Impact of picocell BS density and BS transmit power in a two-tier HCN.

with the MRP cell association R^{UL}_{MRP}, respectively.

Increasing λ_2 improves $P^{UL}_{out,NBS}(R_s)$ and R^{UL}_{NBS} due to the increased harvested energy from the serving nearest BS and the decreased path loss. However, increasing λ_2 to a certain value degrades $P^{UL}_{out,NBS}(R_s)$ and R^{UL}_{NBS} of the macrocell MUs due to the dominant effect of the increased interference from the macrocell MUs with increased transmit power. In contrast, for the MRP cell association, the increase in λ_2 degrades $P^{UL}_{out,MRP}(R_s)$ and R^{UL}_{MRP} of both the tiers due to the dominant effect of higher interference from the large number of other picocell MUs. Furthermore, $P^{DL}_{out,NBS}(R_s)$, R^{DL}_{NBS}, $P^{DL}_{out,MRP}(R_s)$, and R^{DL}_{MRP} are slightly affected by increasing λ_2.

The increase in $P_{t,b}$ in the kth tier improves $P^{UL}_{out,NBS}(R_s)$ and R^{UL}_{NBS} in the kth tier and degrades that in other tiers. The low path loss results in the increased signal power at the BS of its own tier, and the increased interference at the BS of the other tier. The opposite holds true for the MRP cell association, increasing the BS transmit power in the kth tier degrades $P^{UL}_{out,MRP}(R_s)$ and R^{UL}_{MRP} of the kth tier while improves that of other tiers. This is because increasing the BS transmit power in the kth tier results in the increased distance between the MU and the associated BS of the kth tier as opposed to the decrease of the distance between the MU and the associated BS of the other tiers as in (B.1). Increasing BS transmit power only slightly effects $P^{UL}_{out,NBS}(R_s)$, R^{UL}_{NBS}, $P^{UL}_{out,MRP}(R_s)$, and R^{UL}_{MRP} of a random MU in HCNs.

B. Effect of Time Allocation Factor, and Power Splitting Factor on the DL and the UL performance

In this subsection, we examine the effect of the time allocation factor and the power allocation factor on the DL and

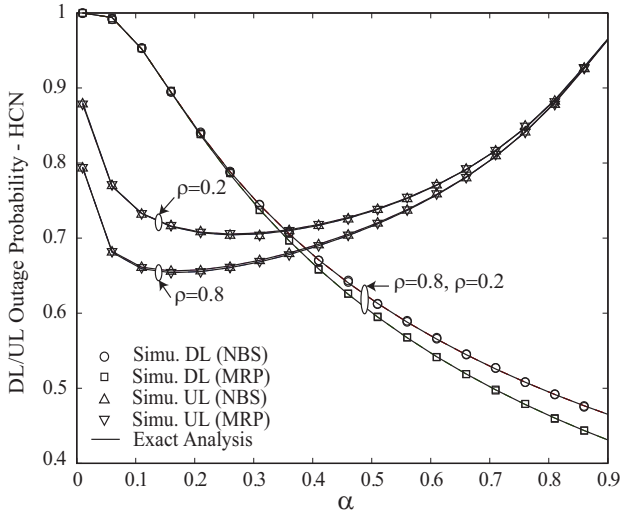

(a) DL/UL outage probability.

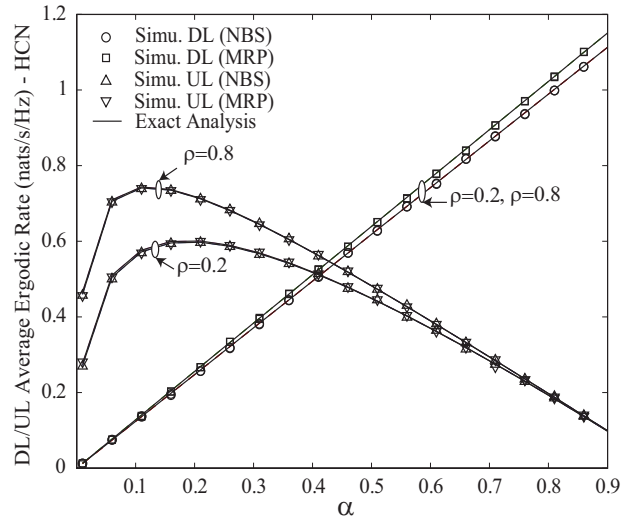

(b) DL/UL average ergodic rate.

Fig. 6: Impact of time allocation factor and power splitting factor on the DL/UL performance in a two-tier HCN.

UL outage probability and average ergodic rate of a random MU in HCNs with the NBS and the MRP cell associations. In Fig. 6, we set $\lambda_1 = 10^{-3}$, $\lambda_2 = 2 \times 10^{-3}$, $P_{t,b_1} = 46$ dBm, and $P_{t,b_2} = 37$ dBm.

Fig. 6a examines the impact of the time allocation factor α and the power splitting factor ρ on the DL and the UL outage probability of a random MU in HCNs with the NBS and the MRP cell associations. Fig. 6b examines the impact of α and ρ on the DL and the UL average ergodic rate of a random MU in HCNs with the NBS and the MRP cell associations. With the increase of α, the DL outage probabilities, $P^{DL}_{out,NBS}(R_s)$ and $P^{DL}_{out,MRP}(R_s)$, and the DL average ergodic rates, R^{DL}_{NBS} and R^{DL}_{MRP}, improve due to allocating large fraction of time to the DL transmission. For the UL performance, first we observe that with the increase in α, the UL outage probabilities, $P^{UL}_{out,NBS}(R_s)$ and $P^{UL}_{out,MRP}(R_s)$, and the UL average ergodic rates, R^{UL}_{NBS} and R^{UL}_{MRP}, improve and then degrade. This is because for small α, the noise plays a dominant role in the $SINR^{UL}_k$ as shown in (6), thus the $SINR^{UL}_k$ increases with increasing α. However, for large α, the degradation of the $P^{UL}_{out,NBS}(R_s)$, R^{UL}_{NBS}, $P^{UL}_{out,MRP}(R_s)$, and R^{UL}_{MRP} is due to allocating a large fraction of time to the DL transmission than to the UL transmission. Interestingly, with the increase of ρ, the DL performance of a random MU in HCNs remains almost unchanged. This is because, with high density of high transmit power BSs, the interference plays a dominant role in the $SINR^{DL}_k$ in (5) and as such the thermal noise is ignored. However, the UL performance of a random MU in HCNs improves by increasing ρ. Transmitting the UL information using a larger fraction of the DL average received power results in the improved UL performance.

C. Effect of Rate Threshold on the DL and the UL performance

Fig. 7 compares the DL and the UL outage probability of a random MU in HCNs with the NBS to that with the MRP cell association. In Fig. 7, we set $\lambda_1 = 10^{-3}$, $\lambda_2 = 2 \times 10^{-3}$, $P_{t,b_1} = 46$ dBm, and $P_{t,b_2} = 37$ dBm.

The DL outage probability of a random MU in HCNs with the MRP cell association is narrowly better than that with the NBS cell association. This is due to the lower aggregate interference in the $SINR^{DL}_k$ with the MRP cell association than that with the NBS cell association. The UL outage probability a random MU in HCNs with the NBS cell association is comparable to that with the MRP cell association.

D. Effect of Power Splitting Factor on the Global Average Ergodic Rate

Fig. 8 examines the impact of power splitting factor ρ on the GL average ergodic rate for the NBS and MRP cell associations using (58). In Fig. 8, we set $\lambda_1 = 10^{-3}$, $\lambda_2 = 2 \times 10^{-3}$, $P_{t,b_1} = 46$ dBm, and $P_{t,b_2} = 37$ dBm.

We observe that the GL average ergodic rate first increases, then decreases with increasing ρ. The increasing trend is due to the increase in the UL average ergodic rate. The sudden decrease is due to the decreases in the DL average ergodic rate. We observe that the optimal power splitting factor ρ^*, that maximizes the GL average ergodic rate, occurs near one, i.e., $\rho^*_{NBS} = 0.999$ and $\rho^*_{MRP} = 0.9995$. Moreover, we observe that the improvement in the GL average ergodic rate for $\rho = 0.4$ to the optimal ρ^* is very small, which reveals that the optimal operation region for ρ is [0.4, 0.999].

VI. Conclusion

We have presented a tractable analytical model of K-tier HCNs with SWIPT where the MUs harvest energy and decode information simultaneously in the DL, and the harvested energy at the MU is then utlized for information transmission in the UL. We have derived the analytical expression for the DL average received power at a random MU with the NBS and the MRP cell associations to demonstrate the effect of

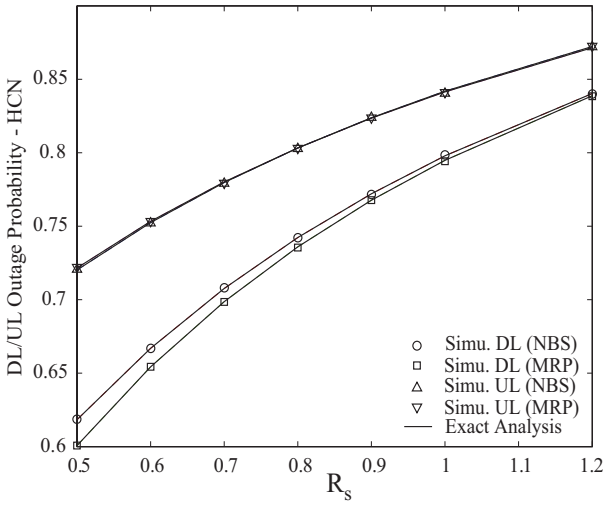

Fig. 7: Impact of rate threshold on the DL/UL outage probability in a two-tier HCN.

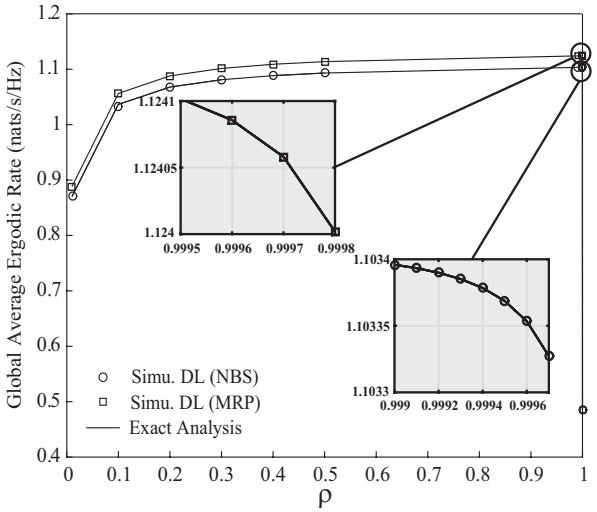

Fig. 8: Impact of power splitting factor on the GL average ergodic rate in a two-tier HCN.

harvested energy on the UL information transmission. We have derived the DL and the UL performance in terms of the outage probability and the average ergodic rate of a random MU in HCNs with the NBS and the MRP cell associations. The DL and UL performance of the NBS cell association is comparable to that of the conventional MRP cell association despite the fact that the UL path loss in the NBS cell association is low. Owing to its simple implementation with low system overheads, the NBS cell association sounds an optimal choice. We have shown that although the harvested energy at the MU can be increased by deploying more small cell BSs and increasing the BS transmit power, the UL performance of a random MU in HCNs with the NBS and the MRP cell associations can not be improved. Nevertheless, the UL performance of a random MU can be improved by increasing the power splitting factor. With the advancements in WPT and interference cancellation, HCNs with SWIPT prove to be promising candidates for 5G systems.

Appendix A
Proof of Lemma 1

We first derive the average value of $I_{b_{\hat{k}}}$ in (4), as follows

$$\begin{aligned}\mathbb{E}[I_{b_{\hat{k}}}] =& \mathbb{E}\left[P_{t,b_{\hat{k}}}|h_{b_{\hat{k}},u_0}|^2 L_0\big(\max\left\{\left\|\boldsymbol{x}_{b_{\hat{k}},u_0}\right\|,d\right\}\big)^{-\ell_k}\right]\\ \overset{(a)}{=}& P_{t,b_{\hat{k}}}L_0\Bigg[\int_0^d d^{-\ell_k} f_{\left\|\boldsymbol{x}_{b_{\hat{k}}}\right\|}(x)dx\\ &+\int_d^\infty x^{-\ell_k} f_{\left\|\boldsymbol{x}_{b_{\hat{k}}}\right\|}(x)dx\Bigg],\end{aligned} \tag{A.1}$$

where (a) follows from the fact that $|h_{b_{\hat{k}}}|^2 \sim exp(1)$. In (A.1), the PDF of $\left\|\boldsymbol{x}_{b_{\hat{k}}}\right\|$ with the NBS cell association is given by [31]

$$f_{\left\|\boldsymbol{x}_{b_{\hat{k}}}\right\|}(x)\big|_{\text{NBS}} = 2\kappa x \exp\{-\kappa x^2\}, \tag{A.2}$$

where κ is given in (13).

Substituting (A.2) into (A.1), and simplifying the resulting equation using [34, eq. 3.381.1] and [34, eq. 3.381.6], we derive $\mathbb{E}[I_{b_{\hat{k}}}]$. Further, the average value of I_{b_x} is derived as

$$\begin{aligned}\mathbb{E}[I_{b_x}] =& \sum_{j=1}^{K}\mathbb{E}_h\left[P_{t,b_j}L_0|h_{b_j u_0}|^2\right]\\ &\mathbb{E}_x\Bigg[\mathbb{E}_{\Phi_j}\Bigg[\sum_{b_j\in\Phi_j\setminus b_{\hat{k}}}\big(\max\left\{\left\|\boldsymbol{x}_{b_j u_o}\right\|,d\right\}\big)^{-\ell_j}\Bigg]\Bigg].\end{aligned} \tag{A.3}$$

The interfering BSs need to be located outside a disc of a radius $r_{min} = \left\|\boldsymbol{x}_{b_{\hat{k}}}\right\| = x$ to satisfy the NBS cell association. Applying the Campbell's Theorem [33] to (A.3), and utilizing the fact that $|h_{b_j u_0}|^2 \sim 1$, we derive

$$\begin{aligned}\mathbb{E}[I_{b_x}] =& \sum_{j=1}^{K} 2\pi P_{t,b_j}L_o\lambda_j\Bigg[\int_0^\infty\Bigg[\int_{r_{min}}^\infty (max\{r,d\})^{-\ell_j} r dr\Bigg]\\ &f_{\left\|\boldsymbol{x}_{b_{\hat{k}}}\right\|}(x)dx\Bigg].\end{aligned} \tag{A.4}$$

Inserting $r_{min} = x$ into (A.4), we have

$$\begin{aligned}\mathbb{E}[I_{b_x}] =& \sum_{j=1}^{K} 2\pi P_{t,b_j}L_o\lambda_j\Bigg[\int_0^d\Big[d^{-\ell_j}\int_x^d r dr + \int_d^\infty r^{-(\ell_j-1)}dr\Big]\\ &f_{\left\|\boldsymbol{x}_{b_{\hat{k}}}\right\|}(x)dx + \int_d^\infty\Big[\int_x^\infty r^{-(\ell_j-1)}dr\Big]f_{\left\|\boldsymbol{x}_{b_{\hat{k}}}\right\|}(x)dx\Bigg].\end{aligned} \tag{A.5}$$

Substituting the PDF of $\left\|\boldsymbol{x}_{b_{\hat{k}}}\right\|$ with NBS cell association from (A.2) into (A.5), and solving the resulting equation by using [34, eq. 3.381.1] and [34, eq. 3.381.6], we obtain $\mathbb{E}[I_{b_x}]$. Combining the equations of $\mathbb{E}[I_{b_{\hat{k}}}]$ and $\mathbb{E}[I_{b_x}]$, we obtain the average received power at the typical kth tier MU with NBS cell association in (7) as Lemma 1.

APPENDIX B
PROOF OF LEMMA 2

We first write the PDF of $\left\|\boldsymbol{x}_{b_{\hat{k}}}\right\|$ with the MRP cell association as given by [31]

$$f_{\left\|\boldsymbol{x}_{b_{\hat{k}}}\right\|}(x)\big|_{\mathrm{MRP}} = \frac{x}{\Upsilon_k}\exp\Big\{-\sum_{j=1}^{K}\mu_{k,j}x^{2\ell_k/\ell_j}\Big\}, \tag{B.1}$$

where Υ_k is given in (20)

The average value of $I_{b_{\hat{k}}}$ is derived by substituting the PDF of $\left\|\boldsymbol{x}_{b_{\hat{k}}}\right\|$ with MRP cell association from (B.1) into (A.1). Further, the average value of I_{b_x} is derived as (A.4) with the interfering BSs located outside the disc of radius $r_{min} = {\delta_{j,k}}^{2/\ell_j}x^{\ell_k/\ell_j}$ to satisfy the MRP cell association. Combining the resulting equations of $\mathbb{E}[I_{b_{\hat{k}}}]$ and $\mathbb{E}[I_{b_x}]$, and finally substituting the PDF of $\left\|\boldsymbol{x}_{b_{\hat{k}}}\right\|$ with the MRP cell association from (B.1) we derive the average received power at the typical kth tier MU with the MRP cell association as Lemma 2.

APPENDIX C
PROOF OF THEOREM 1

According to (5) and (26), the DL outage probability of the typical MU in the kth tier is given as

$$P_{out,k}^{DL}(\beta) = 1 - \int_0^{\infty}\Pr\left[\frac{\left|h_{b_{\hat{k}},\mathrm{u}_0}\right|^2\left\|\boldsymbol{x}_{b_{\hat{k}},\mathrm{u}_0}\right\|^{-\ell_k}}{(I_{b_{x_j}}^{DL}+\sigma^2)\Omega_k^{DL}} > \beta\right] f_{\left\|\boldsymbol{x}_{b_{\hat{k}},\mathrm{u}_0}\right\|}(x)dx, \tag{C.1}$$

where Ω_k^{DL} is given in (30), $I_{b_x}^{DL} = \sum_{b_j\in\Phi_j\setminus b_{\hat{k}}}(1-\rho)P_{t,b_j}\left|h_{b_j,\mathrm{u}_0}\right|^2 L_0\left\|\boldsymbol{x}_{b_j,\mathrm{u}_0}\right\|^{-\ell_j}$, and $f_{\left\|\boldsymbol{x}_{b_{\hat{k}}}\right\|}(x)$ with the NBS cell association is given in (A.2).

In (C.2) the CCDF of a typical MU at a distance x from its associated BS in kth tier is given as

$$\begin{aligned}
&\Pr\left[\frac{\left|h_{b_{\hat{k}},\mathrm{u}_o}\right|^2\left\|\boldsymbol{x}_{b_{\hat{k}},\mathrm{u}_o}\right\|^{-\ell_k}}{(I_{b_x}^{DL}+\sigma^2)\Omega_k^{DL}} > \beta\right]\\
&= \mathbb{E}_{I_{b_x}}\left[\Pr\left[\left|h_{b_{\hat{k}},\mathrm{u}_o}\right|^2 > (I_{b_x}^{DL}+\sigma^2)\beta\Omega_k^{DL}\left\|\boldsymbol{x}_{b_{\hat{k}},\mathrm{u}_o}\right\|^{-\ell_k}\right]\Big|I_{b_x}^{DL}\right]\\
&\overset{(a)}{=}\int_0^{\infty}\exp\left\{-\left(\Omega^{DL}+\sigma^2\right)\beta\Omega_k^{DL}\left\|\boldsymbol{x}_{b_{\hat{k}},\mathrm{u}_o}\right\|^{-\ell_k}\right\}\\
&\quad dPr\left(I_{b_x}^{DL}\le\Omega^{DL}\right)\\
&\overset{(b)}{=}\exp\left\{-\sigma^2\beta\Omega_k^{DL}\left\|\boldsymbol{x}_{b_{\hat{k}},\mathrm{u}_o}\right\|^{\ell_k}\right\}\mathcal{L}_{I_{b_x}^{DL}}\left(\beta\Omega_k^{DL}\left\|\boldsymbol{x}_{b_{\hat{k}},\mathrm{u}_0}\right\|^{-\ell_k}\right),
\end{aligned} \tag{C.2}$$

where (a) follows from the fact that $|h_{b_{\hat{k}}u_0}|^2 \sim 1$, and (b) follows from the definition of Laplace transform of interference $\mathcal{L}_{I_{b_x}^{DL}}(s) = \int_x^{\infty}\exp\left(-s\Omega^{DL}\right)dPr\left(I_{b_x}^{DL}\le\Omega^{DL}\right)$, where the integration limit follows from the fact that the nearest interferer in jth tier is at least at $r_{min}=x$. Using generating functional of HPPP in [33] $\mathcal{L}_{I_{b_x}^{DL}}(s)$ is given as

$$\begin{aligned}
\mathcal{L}_{I_{b_x}^{DL}}(s) &= \exp\Big\{2\pi\sum_{j=1}^{K}\lambda_j\int_x^{\infty}\Big(1-\mathbb{E}_h\big[-s(1-\rho)P_{t,b_j}\left|h_{b_j,\mathrm{u}_0}\right|^2 L_0\left\|\boldsymbol{x}_{b_j,\mathrm{u}_0}\right\|^{-\ell_j}\big]\Big)ydy\Big\}\\
&\overset{(a)}{=}\exp\Big\{2\pi\sum_{j=1}^{K}\lambda_j\int_x^{\infty}\big(1-\frac{1}{1+\mho_{k,j}y^{-\ell_j}}\big)ydy\Big\}
\end{aligned} \tag{C.3}$$

$$= \exp\Big\{-\sum_{j=1}^{k}\pi\lambda_j\vartheta_{k,j}\Big\}, \tag{C.4}$$

where (a) follows from the fact that $|h_{b_j u_0}|^2 \sim 1$ and $\mho_{j,k}$ is given in (31). Simplifying (C.3) by employing change of variables $z = \mho_{k,j}^{-2/\ell_j}y^2$ we derive (C.4) where $\vartheta_{k,j}$ is given in (29). Substituting (C.4) into (C.2), we derive,

$$\Pr\left(SINR_k^{DL}\left(\left\|\boldsymbol{x}_{b_{\hat{k}},\mathrm{u}_0}\right\|\right) > \beta\right) = \exp\Big\{-\sigma^2\beta\Omega_k^{DL}\left\|\boldsymbol{x}_{b_{\hat{k}},\mathrm{u}_o}\right\|^{\ell_k} - \sum_{j=1}^{k}\pi\lambda_j\vartheta_{k,j}\Big\} \tag{C.5}$$

Finally plugging (C.5) and (A.2) into (C.1), we obtain Theorem 1.

APPENDIX D
PROOF OF THEOREM 2

For the MRP cell association, the Laplace transform in (C.2) is evaluated with lower integration limit $r_{min} = {\delta_{j,k}}^{2/\ell_j}x^{\ell_k/\ell_j}$ by utilizing the fact that the nearest interferer in the jth tier is at least at ${\delta_{j,k}}^{2/\ell_j}x^{\ell_k/\ell_j}$. Then following the similar steps as of Theorem 1 with the PDF of $\left\|\boldsymbol{x}_{b_{\hat{k}}}\right\|$ for the MRP cell association given in (B.1), we derive Theorem 2.

APPENDIX E
PROOF OF THEOREM 3

Based on (53), the DL average ergodic rate of a typical MU associated with the kth tier using NBS cell association is derived as

$$\begin{aligned}
R_k^{DL} &= \int_0^{\infty}\mathbb{E}_{SINR_k^{DL}}\left[\alpha\ln\left(1+SINR_k^{DL}(x)\right)\right]f_{\left\|\boldsymbol{x}_{b_{\hat{k}},\mathrm{u}_0}\right\|}(x)dx\\
&= \int_0^{\infty}\int_0^{\infty}\Pr\left[SINR_k^{DL}(x) > (e^{t/\alpha}-1)\right]dtf_{\left\|\boldsymbol{x}_{b_{\hat{k}},\mathrm{u}_0}\right\|}(x)dx.
\end{aligned} \tag{E.1}$$

Simplifying (E.1) as of (C.5) and substituting (A.2), we obtain Theorem 3.

APPENDIX F
PROOF OF THEOREM 4

The DL average ergodic rate of a typical MU associated with the kth tier using MRP cell association is derived by simplifying (E.1) following the similar steps as of Theorem 2 for the MRP cell association and substituting (B.1).

REFERENCES

[1] S. Akbar, Y. Deng, A. Nallanathan, and M. Elkashlan, "Downlink and uplink transmission in K-tier heterogeneous cellular network with simultaneous wireless information and power transfer," in *IEEE Global Commun. Conf. (GLOBECOM)*, Dec. 2015, pp. 1–6.

[2] P. Demestichas, A. Georgakopoulos, D. Karvounas, K. Tsagkaris, V. Stavroulaki, J. Lu, C. Xiong, and J. Yao, "5G on the horizon: Key challenges for the radio-access network," *IEEE Trans. Veh. Technol.*, vol. 8, no. 3, pp. 47–53, Sept. 2013.

[3] R. Hu and Y. Qian, "An energy efficient and spectrum efficient wireless heterogeneous network framework for 5G systems," *IEEE Commun. Mag.*, vol. 52, no. 5, pp. 94–101, May 2014.

[4] J. Andrews, S. Buzzi, W. Choi, S. Hanly, A. Lozano, A. Soong, and J. Zhang, "What will 5G be?" *IEEE J. Sel. Areas Commun.*, vol. 32, no. 6, pp. 1065–1082, June 2014.

[5] X. Lu, P. Wang, D. Niyato, D. I. Kim, and Z. Han, "Wireless networks with RF energy harvesting: A contemporary survey," *IEEE Commun. Surveys Tuts.*, vol. 17, no. 2, pp. 757–789, Secondquarter 2015.

[6] S. Bi, C. Ho, and R. Zhang, "Wireless powered communication: opportunities and challenges," *IEEE Commun. Mag.*, vol. 53, no. 4, pp. 117–125, Apr. 2015.

[7] I. Krikidis, S. Timotheou, S. Nikolaou, G. Zheng, D. Ng, and R. Schober, "Simultaneous wireless information and power transfer in modern communication systems," *IEEE Commun. Mag.*, vol. 52, no. 11, pp. 104–110, Nov. 2014.

[8] K. Huang and E. Larsson, "Simultaneous information and power transfer for broadband wireless systems," *IEEE Trans. Signal Process.*, vol. 61, no. 23, pp. 5972–5986, Dec. 2013.

[9] S. Parkvall, A. Furuskar, and E. Dahlman, "Evolution of lte toward imt-advanced," *IEEE Commun. Mag.*, vol. 49, no. 2, pp. 84–91, Feb. 2011.

[10] A. Khandekar, N. Bhushan, J. Tingfang, and V. Vanghi, "Lte-advanced: Heterogeneous networks," in *European Wireless Conference (EW)*, Apr. 2010, pp. 978–982.

[11] D. Liu, Y. Chen, K. K. Chai, T. Zhang, and M. Elkashlan, "Opportunistic user association for multi-service hetnets using nash bargaining solution," *IEEE Commun. Lett.*, vol. 18, no. 3, pp. 463–466, Mar. 2014.

[12] R. Madan, J. Borran, A. Sampath, N. Bhushan, A. Khandekar, and T. Ji, "Cell association and interference coordination in heterogeneous LTE-A cellular networks," *IEEE J. Sel. Areas Commun.*, vol. 28, no. 9, pp. 1479–1489, Dec. 2010.

[13] A. Ghosh, N. Mangalvedhe, R. Ratasuk, B. Mondal, M. Cudak, E. Visotsky, T. A. Thomas, J. G. Andrews, P. Xia, H. S. Jo, H. S. Dhillon, and T. D. Novlan, "Heterogeneous cellular networks: From theory to practice," *IEEE Commun. Mag.*, vol. 50, no. 6, pp. 54–64, June 2012.

[14] J. G. Andrews, H. Claussen, M. Dohler, S. Rangan, and M. C. Reed, "Femtocells: Past, present, and future," *IEEE J. Sel. Areas Commun.*, vol. 30, no. 3, pp. 497–508, Apr. 2012.

[15] H. Ju and R. Zhang, "Throughput maximization in wireless powered communication networks," *IEEE Trans. Commun.*, vol. 13, no. 1, pp. 418–428, Jan. 2014.

[16] L. Liu, R. Zhang, and K.-C. Chua, "Multi-antenna wireless powered communication with energy beamforming," *IEEE Trans. Commun.*, vol. 62, no. 12, pp. 4349–4361, Dec. 2014.

[17] H. Ju and R. Zhang, "User cooperation in wireless powered communication networks," in *2014 IEEE Global Commun. Conf. (GLOBECOM)*, Dec. 2014, pp. 1430–1435.

[18] X. Kang, C. Ho, and S. Sun, "Full-duplex wireless-powered communication network with energy causality," *IEEE Trans. Wireless Commun.*, vol. 14, no. 10, pp. 5539–5551, Oct. 2015.

[19] G. Yang, C. K. Ho, R. Zhang, and Y. L. Guan, "Throughput optimization for massive mimo systems powered by wireless energy transfer," *IEEE J. Sel. Areas Commun.*, vol. 33, no. 8, pp. 1640–1650, Aug. 2015.

[20] Y. Liu, S. A. Mousavifar, Y. Deng, C. Leung, and M. Elkashlan, "Wireless energy harvesting in a cognitive relay network," *IEEE Trans. Wireless Commun.*, vol. 15, no. 4, pp. 2498–2508, Apr. 2016.

[21] S. Lee, R. Zhang, and K. Huang, "Opportunistic wireless energy harvesting in cognitive radio networks," *IEEE Trans. Wireless Commun.*, vol. 12, no. 9, pp. 4788–4799, Sept. 2013.

[22] A. H. Sakr and E. Hossain, "Cognitive and energy harvesting-based D2D communication in cellular networks: Stochastic geometry modeling and analysis," *IEEE Trans. Commun.*, vol. 63, no. 5, pp. 1867–1880, May 2015.

[23] K. Huang and V. K. N. Lau, "Enabling wireless power transfer in cellular networks: Architecture, modeling and deployment," *CoRR*, 2012. [Online]. Available: http://arxiv.org/abs/1207.5640

[24] Y. Deng, L. Wang, M. Elkashlan, M. D. Renzo, and J. Yuan, "K-tier heterogeneous cellular networks with wireless power transfer," in *IEEE Int. Commun. Conf. (ICC)*, May 2016.

[25] A. Sakr and E. Hossain, "Analysis of multi-tier uplink cellular networks with energy harvesting and flexible cell association," in *IEEE Global Commun. Conf. (GLOBECOM)*, Dec. 2014, pp. 4525–4530.

[26] K. Huang and X. Zhou, "Cutting last wires for mobile communication by microwave power transfer," *CoRR*, vol. abs/1408.3198, 2014. [Online]. Available: http://arxiv.org/abs/1408.3198

[27] H. ElSawy, E. Hossain, and M. Haenggi, "Stochastic geometry for modeling, analysis, and design of multi-tier and cognitive cellular wireless networks: A survey," *IEEE Commun. Surveys and Tutorials*, vol. 15, no. 3, pp. 996–1019, 2013.

[28] D. Liu, L. Wang, Y. Chen, M. Elkashlan, K. K. Wong, R. Schober, and L. Hanzo, "User association in 5g networks: A survey and an outlook," *IEEE Commun. Surveys Tuts.*, vol. PP, no. 99, pp. 1–1, 2016.

[29] A. Sakr and E. Hossain, "Analysis of K-tier uplink cellular networks with ambient RF energy harvesting," *IEEE J. Sel. Areas Commun.*, vol. 33, no. 10, pp. 2226–2238, Oct. 2015.

[30] F. Boccardi, J. Andrews, H. Elshaer, M. Dohler, S. Parkvall, P. Popovski, and S. Singh, "Why to decouple the uplink and downlink in cellular networks and how to do it," *IEEE Commun. Mag.*, vol. 54, no. 3, pp. 110–117, Mar. 2016.

[31] H.-S. Jo, Y. J. Sang, P. Xia, and J. G. Andrews, "Heterogeneous cellular networks with flexible cell association: A comprehensive downlink SINR analysis," *IEEE Trans. Wireless Commun.*, vol. 11, no. 10, pp. 3484–3495, Oct. 2012.

[32] F. Baccelli, B. Blaszczyszyn, and P. Muhlethaler, "An aloha protocol for multihop mobile wireless networks," *IEEE Trans. Inf. Theory*, vol. 52, no. 2, pp. 421–436, Feb. 2006.

[33] D. Stoyan, W. Kendall, and J. Mecke, "Stochastic geometry and its applications," *Wiley New York*, vol. 2, 1987.

[34] I. S. Gradshteyn and I. M. Ryzhik, *Table of Integrals, Series and Products*, 7th ed. San Diego, C.A.: Academic Press, 2007.

Sunila Akbar (S'15) received the B.E degree in Electrical Engineering from NED University of Engg. and Tech. (NEDUET), Karachi, Pakistan, in 1998. She then worked as a Projects Coordinator for the Electrical Division at a local Contracting Company in Dubai, UAE, for five years before joining NEDUET as a Lecturer in 2004. In 2007, she completed M.Engg degree in Telecommunications Engineering from NEDUET and appointed as an Assistant Professor at the same in 2008. She is currently working towards the PhD degree in the Department of Informatics, King's College London, UK. Ms. Akbar has been a reviewer in several IEEE conferences. Her current research interests include statistical modeling of wireless networks, heterogeneous cellular networks, massive MIMO, and energy efficient communications.

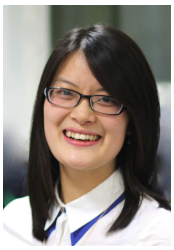

Yansha Deng (M'16) received the Ph.D. degree in Electrical Engineering from Queen Mary University of London, UK, 2015. She is currently the postdoctoral research fellow in the Department of Informatics, at King's College London, UK.

Her research interests include massive MIMO, HetNets, molecular communication, cognitive radio, cooperative networks, and physical layer security. She has served as TPC member for many IEEE conferences such as IEEE GLOBECOM and ICC.

Arumugam Nallanathan (S'97–M'00–SM'05) is a Professor of Wireless Communications in the Department of Informatics at King's College London (University of London). He served as the Head of Graduate Studies in the School of Natural and Mathematical Sciences at King's College London, 2011–2012. He was an Assistant Professor in the Department of Electrical and Computer Engineering, National University of Singapore from August 2000 to December 2007. His research interests include 5G Technologies, Millimeter wave communications, Cognitive Radio and Relay Networks. In these areas, he co-authored more than 250 papers. He is a co-recipient of the Best Paper Award presented at the 2007 IEEE International Conference on Ultra-Wideband (ICUWB'2007). He is an IEEE Distinguished Lecturer. He is an Editor for IEEE TRANSACTIONS ON COMMUNICATIONS and IEEE TRANSACTIONS ON VEHICULAR TECHNOLOGY. He was an Editor for IEEE TRANSACTIONS ON WIRELESS COMMUNICATIONS (2006–2011), IEEE WIRELESS COMMUNICATIONS LETTERS and IEEE SIGNAL PROCESSING LETTERS. He served as the Chair for the Signal Processing and Communication Electronics Technical Committee of IEEE Communications Society, Technical Program Co-Chair (MAC track) for IEEE WCNC 2014, Co-Chair for the IEEE GLOBECOM 2013 (Communications Theory Symposium), Co-Chair for the IEEE ICC 2012 (Signal Processing for Communications Symposium), Co-Chair for the IEEE GLOBECOM 2011 (Signal Processing for Communications Symposium), Technical Program Co-Chair for the IEEE International Conference on UWB 2011 (IEEE ICUWB 2011), Co-Chair for the IEEE ICC 2009 (Wireless Communications Symposium), Co-Chair for the IEEE GLOBECOM 2008 (Signal Processing for Communications Symposium) and General Track Chair for IEEE VTC 2008. He received the IEEE Communications Society SPCE outstanding service award 2012 and IEEE Communications Society RCC outstanding service award 2014.

Maged Elkashlan (M'06) received the Ph.D. degree in Electrical Engineering from the University of British Columbia, Canada, 2006. From 2007 to 2011, he was with the Wireless and Networking Technologies Laboratory at Commonwealth Scientific and Industrial Research Organization (CSIRO), Australia. During this time, he held an adjunct appointment at University of Technology Sydney, Australia. In 2011, he joined the School of Electronic Engineering and Computer Science at Queen Mary University of London, UK. He also holds visiting faculty appointments at the University of New South Wales, Australia, and Beijing University of Posts and Telecommunications, China. His research interests fall into the broad areas of communication theory, wireless communications, and statistical signal processing for distributed data processing, heterogeneous networks, and Massive MIMO.

Dr. Elkashlan currently serves as Editor of IEEE TRANSACTIONS ON WIRELESS COMMUNICATIONS, IEEE TRANSACTIONS ON VEHICULAR TECHNOLOGY, and IEEE COMMUNICATIONS LETTERS. He also serves as Lead Guest Editor for the special issue on "Green Media: The Future of Wireless Multimedia Networks" of the IEEE WIRELESS COMMUNICATIONS MAGAZINE, Lead Guest Editor for the special issue on "Millimeter Wave Communications for 5G" of the IEEE COMMUNICATIONS MAGAZINE, Guest Editor for the special issue on "Energy Harvesting Communications" of the IEEE COMMUNICATIONS MAGAZINE, and Guest Editor for the special issue on "Location Awareness for Radios and Networks" of the IEEE JOURNAL ON SELECTED AREAS IN COMMUNICATIONS. He received the Best Paper Award at the IEEE International Conference on Communications (ICC) in 2014, the International Conference on Communications and Networking in China (CHINACOM) in 2014, and the IEEE Vehicular Technology Conference (VTC-Spring) in 2013. He received the Exemplary Reviewer Certificate of the IEEE Communications Letters in 2012.

Abdol-Hamid Aghvami (M'89–SM'91–F'05) is a Professor of telecommunications engineering at King's College London. He has published over 600 technical papers and given invited talks and courses worldwide on various aspects of personal and mobile radio communications. He was Visiting Professor at NTT Radio Communication Systems Laboratories in 1990, Senior Research Fellow at BT Laboratories in 1998–1999, and was an Executive Advisor to Wireless Facilities Inc., USA, in 1996–2002. He was a member of the Board of Governors of the IEEE Communications Society in 2001–2003, was a Distinguished Lecturer of the IEEE Communications Society in 2004–2007, and has been member, Chairman, and Vice-Chairman of the technical programme and organising committees of a large number of international conferences. He is also the founder of International Symposium on Personal Indoor and Mobile Radio Communications (PIMRC), a major yearly conference attracting nearly 1000 attendees. Dr. Aghvami was awarded the IEEE Technical Committee on Personal Communications (TCPC) Recognition Award in 2005 for his outstanding technical contributions to the communications field, and for his service to the scientific and engineering communities. He is a Fellow of the Royal Academy of Engineering, Fellow of the IET, and in 2009 was awarded a Fellowship of the Wireless World Research Forum in recognition of his personal contributions to the wireless world.